Proposal for a Procedure for Measuring the Transverse Dimensions of a Beam of Relativistic Electrons with a Small Longitudinal Size

I. E. Vnukov[a], *, Yu. A. Goponov[a], S. A. Laktionova[a], R. A. Shatokhin[a],
K. Sumitani[b], and Y. Takabayashi[c]

[a]*Belgorod National Research University, Belgorod, 308015 Russia*
[b]*Japan Synchrotron Radiation Research Institute (JASRI), 1-1-1 Kouto, Sayo-cho, Sayo-gun, Hyogo 679-5198, Japan*
[c]*SAGA Light Source, Tosu, Saga 841-0005, Japan*
*e-mail: vnukov@bsu.edu.ru

Abstract—The possibility of implementing a previously proposed procedure for determining the beam dimensions at a target is analyzed; it includes the measurement of two-dimensional angular distributions of the coherent radiation of fast electrons for two distances between a crystal, where radiation is generated, and a coordinate detector. The use of two mechanisms of parametric X-ray radiation and diffracted transition radiation is considered. The limits of the method sensitivity and the influence of the departure of secondary electrons and photons on them are discussed.

INTRODUCTION

The divergence of the electron beam and its transverse dimensions are ones of the most important parameters of any accelerator. A large number of different procedures, including the use of wire scanners and fluorescent screens, have been developed to measure them [1, 2]. Optical radiation produced during particle propagation through thin metal plates or near them, namely, optical transition radiation (OTR) [3] and optical diffraction radiation (ODR) [4], respectively, is widely used for accelerators. However, as was shown recently, it is impossible to use OTR to measure the profiles of electron beams of linear accelerators used to create an X-ray free electron laser (XFEL), because OTR becomes coherent in the case where the longitudinal size of the electron bunch is comparable with the wavelength of the recorded radiation [5].

The coherence effect can be avoided if radiation with a wavelength that is smaller than the characteristic bunch dimensions, in particular, the parametric X-ray radiation (PXR) of electrons in crystals, is used [6, 7]. Measurements of the angular distributions of the PXR of fast electrons in thin crystals by means of coordinate detectors [7–9] confirmed the possibility of determining the beam dimensions (by a detector located in the immediate vicinity of the crystal [7]) and changes in the forms of recorded distributions as functions of the beam dimensions for the crystal [8]. The possibility of determining the dimensions of the beam of particles at the target by means of a camera obscura was also shown in [9].

It is not always possible to locate the coordinate detector in the immediate vicinity of the radiation source [7]. In addition, the problem of separating the recorded angular distribution from the bremsstrahlung background, the source of which includes components of the accelerator construction, arises. The use of a camera obscura [9] requires a considerable amount of time to conduct measurements because of strict radiation collimation and suggests azimuthal symmetry of the angular distribution of the recorded radiation. As was noted in the cited paper, the invalidity of this condition leads to a systematic error in the results of measuring the electron-beam dimensions at the target.

The authors of [10] using the approach in [11] developed a procedure taking into account the influence of the transverse dimensions of the particle beam at the target on the recorded angular distribution for three mechanisms of the generation of coherent radiation during the interaction of fast electrons with crystals: PXR, diffraction bremsstrahlung (DB), and diffracted transition radiation (DTR). Comparison of the calculated results with the experimental data [12, 13] showed good agreement and confirmed the adequacy of the developed procedure. The analysis given in the cited paper showed that the measurement of one-dimensional angular distributions cannot provide the required accuracy of determination of the dimensions

of the particle beam at the crystal because of a systematic error caused by the mutual influence of the beam dimensions in a plane on the results of measuring the angular distribution in another plane.

To solve this problem, it is proposed that the size of the electron beam be determined in both planes using the results of measuring the two-dimensional angular distributions of the coherent radiation of electrons in a thin crystal for two distances between the crystal, where the recorded radiation is generated, and a coordinate detector by means of the least squares method. To prove the operating capacity of the method, the author of the cited paper [10] used a model angular distribution that is close to the angular PXR distribution, but not coinciding with it, which made it impossible to reliably determine the limits of the method sensitivity and applicability range.

Proceeding from the foregoing, determination of the sensitivity of the proposed method and the limits of its applicability range is important and urgent.

TAKING INTO ACCOUNT THE SPATIAL DIMENSIONS OF THE ELECTRON BEAM

We present a brief description of the procedure for estimating the electron-beam size, following [10]. The influence of the beam dimensions and the distance between the crystal and the detector on the measured two-dimensional angular distribution of coherent radiation, for example, [7], can be described by the following expression:

$$
\begin{aligned}
& Y(\theta'_x, \theta'_y) \\
& = \iint Y(\theta_y, \theta_x) G(\theta_y \to \theta'_y, \theta_x \to \theta'_x) d\theta_y d\theta_x,
\end{aligned}
\tag{1}
$$

where $Y(\theta'_y, \theta'_x)$ and $Y(\theta_y, \theta_x)$ are the angular distributions of coherent radiation for extended and point beams of particles at the target; integration is performed within the limits of the full solid angle. The function $G(\theta_y \to \theta'_y, \theta_x \to \theta'_x)$ describes the relation between the variables of each of these distributions in the case of the spread of points of electron incidence for the crystal and can be represented in the following form for the two-dimensional Gaussian distribution of such a spread:

$$
\begin{aligned}
& G(\theta_y \to \theta'_y, \theta_x \to \theta'_x) \\
& = \frac{R^2}{2\pi\sigma_y\sigma_x} \exp\left(\frac{-R^2(\theta_y - \theta'_y)^2}{2\sigma_y^2}\right) \exp\left(\frac{-R^2(\theta_x - \theta'_x)^2}{2\sigma_x^2}\right),
\end{aligned}
\tag{2}
$$

where σ_x, σ_y are the characteristic dimensions of the beam in the horizontal and vertical planes and R is the crystal−detector distance. As is seen from the given expressions, the change in the crystal−detector distance leads to that in the recorded angular radiation distribution, which can be used to determine the beam

size by comparing the angular distributions for different crystal—detector distances.

It is necessary to pass to two-dimensional distributions because of the unavoidable problem of the mutual influence of the dimensions in both planes on the distribution of the radiation intensities in these directions. For a detector located at the distance R, on the basis of expression (1), the two-dimensional distribution of the radiation intensity $Y_R(\theta_{y_i}, \theta_{x_j})$ measured by it can be written in the following form:

$$
Y_R(\theta_{y_i}, \theta_{x_j}) = \iint_{\Delta\Omega(y_i, x_j)} Y_R(\theta'_y, \theta'_x) d\theta'_y d\theta'_x,
\tag{3}
$$

where $Y(\theta'_y, \theta'_x)$ is the convolution of the intrinsic angular radiation distribution and the Gaussian one, whose parameters are determined by the beam dimensions and the crystal—detector distance in accordance with expressions (1) and (2). $\Delta\Omega(y_i, x_j)$ is the solid angle covered by the component of the coordinate detector located at the point y_i, x_j, integration is performed over it.
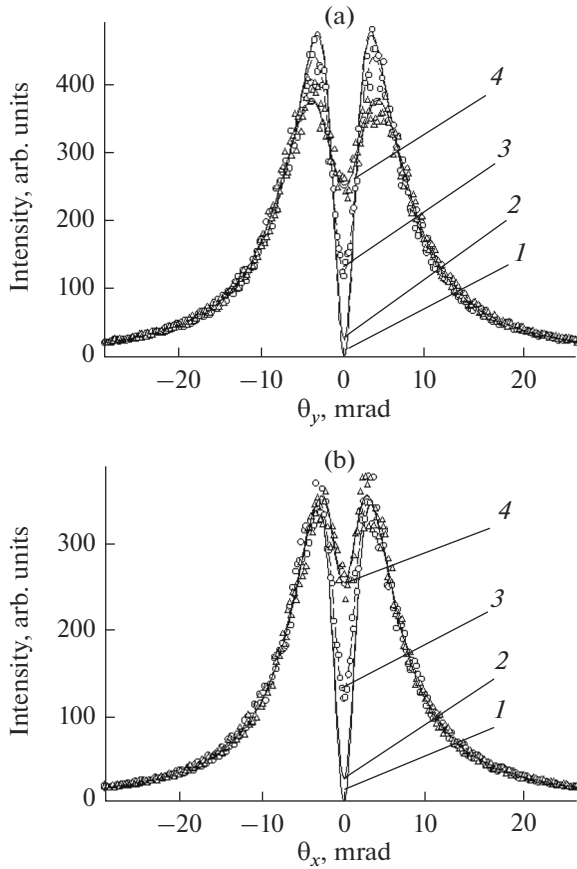
It is obvious that the difference between the distributions $Y_{R_1}(\theta'_{y_i}, \theta'_{x_j})$ and $Y_{R_2}(\theta'_{y_i}, \theta'_{x_j})$, measured for the distances R_1 and R_2 is only due to the characteristic beam dimensions and the crystal—detector distances. And these distributions are the result of convolution of the angular distribution for a point particle beam $Y(\theta_y, \theta_x)$ and two two-dimensional Gaussian distributions with the standard deviations $\sigma'_{x_1, y_1} = \sigma_{x,y}/R_1$ and $\sigma'_{x_2, y_2} = \sigma_{x,y}/R_2$, where $\sigma_{x,y}$ are the characteristic beam dimensions for the crystal.

We assume that $R_1 = k \times R_2$, where k is a coefficient significantly differing from unity, and the solid angles covered by the detectors in each measurement are the same. Thus, for each of the distances, the detector component dimensions differ by k times. In this case, in the first approximation, it can be assumed that $Y_{R_2}(\theta'_{y_i}, \theta'_{x_j})$ is the convolution of the distribution $Y_{R_1}(\theta'_{y_i}, \theta'_{x_j})$ and the Gaussian one with a dispersion that is dependent on unknown beam dimensions at the target and on R_1 and R_2.

To determine the sought beam dimensions at the target, it is possible to use the method of least squares by minimizing the quadratic form:

$$
\begin{aligned}
& \sum_{i=1}^{n}\sum_{j=1}^{m}\left[Y(\theta_{y_i}, \theta_{x_j})_{R_2} - \frac{1}{2\pi\sigma'_x\sigma'_y}\sum_{i'=1}^{n}\sum_{j'=1}^{m} Y(\theta_{y_i}, \theta_{x_j})_{R_1} \right. \\
& \left. \times \exp\left(-\frac{(\theta_{y_i} - \theta_{x_{i'}})^2}{2(\sigma'_y)^2}\right) \exp\left(-\frac{(\theta_{x_i} - \theta_{x_{j'}})^2}{2(\sigma'_x)^2}\right) \right]^2 = \text{Min},
\end{aligned}
\tag{4}
$$

Fig. 1. (a) Vertical and (b) horizontal angular PXR distributions. The curves correspond to (*1*) the Feranchuk—Ivashin distribution, (*2*) the distribution for the point electron beam, (*3*) the distribution for the extended beam and a distance of 1 m, and (*4*) the distribution for the extended beam and a distance of 0.5 m. The points correspond to a distance of 1 m; and triangles, to a distance of 0.5 m.

where *m* and *n* are the numbers of points of the measured distributions in the horizontal and vertical directions, and σ'_x and σ'_y are the fitting parameters minimizing this form and related to the beam dimensions at the target $\tilde{\sigma}_x, \tilde{\sigma}_y$ as follows:

$$\tilde{\sigma}_{x,y} \approx \frac{k \times R_2}{\sqrt{k^2 - 1}} \sigma'_{x,y}. \tag{5}$$

To verify the procedure and to determine the limits of its applicability, we simulate the determination of the beam dimensions from two-dimensional PXR distributions using a variation of the convolution parameters in combination with the gradient-descent method. Simulation was carried out under experimental conditions [12] including a Si crystal with the reflecting (011) plane and an observation angle of 32.2°. The characteristic angle of PXR photon escape was

$$\Theta_{ph} = \sqrt{\gamma^{-2} + \frac{\omega_p^2}{\omega^2}} = 3.32 \text{ mrad, where } \gamma \text{ is the Lorentz}$$

factor and $\omega = 11.65$ keV and $\omega_p = 30.8$ eV are the photon energy and the plasmon energy of the medium. The electron energy was 255 MeV. The dimensions of the detector components were 0.1 and 0.2 mm in both directions for distances of 0.5 and 1 m, respectively. The dimensions of the electron beams at the crystal were $\sigma_x = 0.3$ mm and $\sigma_y = 0.8$ mm. Figure 1 shows the vertical (Fig. 1a) and horizontal (Fig. 1b) angular distributions passing through the reflection center. The Feranchuk—Ivashin formula [14]

$$Y_{PXR}(\theta_x, \theta_y) = N_{PXR}(\omega) \frac{\theta_x^2 \cos^2 2\Theta_B + \theta_y^2}{\left(\theta_x^2 + \theta_y^2 + \Theta_{ph}^2\right)^2}. \tag{6}$$

was used as the model PXR distribution (dependence *1*). Here, $N_{PXR}(\omega)$ is a factor, which characterized the PXR yield and Θ_B is the angle of crystal-plane rotation with respect to the electron-beam direction.

To obtain the angular distribution from the point electron beam (dependence *2*), the angular PXR distribution was convolved with the two-dimensional Gaussian one with $\theta_e = 0.3$ mrad, where θ_e is the divergence of the electron beam. Under these conditions, the contribution of the diffraction of actual photons did not exceed 10% [11]; and therefore, it was not taken into account. Dependences *3* and *4* correspond to an extended electron beam for distances of $R_1 = 2R_2 = 1$ m and $R_2 = 0.5$ m. To take into account the possible influence of the statistical straggling of the measurement results, dependence *3* and *4* were made "noisy" using the uniform distribution in the range of values of ±10% at each point (points and triangles, respectively).

The error in determining the fitting parameters and estimating the beam dimensions obtained from it did not exceed several percent. The dependence obtained as a result of fitting almost coincides with dependence *4* and, therefore, is not given here.

To determine the method sensitivity and applicability limits, we perform a cycle of estimations of the beam dimensions obtained using this procedure and of "noisy" angular distributions as functions of crystal—detector distances. Simulation was performed for beam dimensions of $\sigma_x = 0.3$ mm and $\sigma_y = 0.8$ mm. The other parameters coincided with those described above. The dependence of estimation of the beam size $\tilde{\sigma}_{x,y}$ on the distance obtained as a result of fitting is given in Fig. 2. We took standard deviations of the values obtained as a result of fitting from the average one as errors. As before, we assume that the condition $R_1 = 2R_2$ is satisfied.

It is seen from Fig. 2 that, for R_2 which are smaller than 1.5 m, the error in determining the beam size does not exceed 5−7%, and the values obtained as a result of fitting coincide with those used in the simulation. However, for large distances, $\tilde{\sigma}_x$ differs from

the true value, while $\tilde{\sigma}_y$, coincides with the value used in the simulation process as before, $\sigma_y = 0.8$ mm.

Analysis showed that the reason is a decrease in the difference between the dependences $Y_1(\theta_{y_i}, \theta_{x_j})$ and $Y_2(\theta_{y_i}, \theta_{x_j})$ with increasing distance; therefore, for large R_2, the method loses its sensitivity. The criterion for the absence of a difference can be assumed to be the ratio of $\sigma' = \dfrac{\sigma}{R_2} < 0.3$ mrad to the characteristic angle $\Theta_{ph} = 3.32$ mrad, i.e., $\dfrac{\sigma'}{\Theta_{ph}} < 0.1$.

Assuming that the observation angle and the crystal—detector distance in the experiment [8] are close to the limiting values, we can estimate the minimum beam size available for the measurement using the proposed method. The distance between the crystal and the detector located at an angle of 22.5° was 350 mm. For smaller distances and observation angles, the distance between the beam axis and the detector center is smaller than 10 cm, which makes it impossible to place the detector with protection at this point.

Hence, using the criterion $\sigma \sim 0.1R \times \Theta_{ph}$, where $\Theta_{ph} = 1.54$ mrad, we obtain that the minimum beam size that can be estimated using the proposed procedure is on the order of 60 μm.

Thus, the procedure based on measuring the angular PXR distributions for two distances can provide the measurement of a beam size of ~100 μm and more, which is typical of accelerators of medium energies. However, it cannot be applied to measure transverse beam dimensions on the order of several tens of microns in fourth-generation radiation sources [15], precisely for which the problem of measurement of the spatial dimensions of electron bunches with small longitudinal dimensions arose [5].

As shown in [16] and was confirmed in [17, 18], the contribution of transition-radiation diffraction at the reflection center becomes much larger than that of PXR as the electron energy increases to 5 GeV. For an electron energy of 10 GeV, the angular density of DTR exceeds that of PXR by a factor of 500 or more because of a sharp decrease in the characteristic radiation angle γ^{-1}, determining the angular distribution of the transition radiation, and, consequently, of DTR. Therefore, the PXR contribution at the center of the angular radiation distribution can be assumed to be negligibly small.

The presence of the bright peak in the angular radiation distribution [16, 23], whose form is like that of the angular PXR distribution, in Figs. 1 and 3, makes it possible also to use the above procedure to determine the dimensions of a high-energy electron beam. In this case, the characteristic angle of the radiation yield is close to γ^{-1}, i.e., it turns out to be ten times or
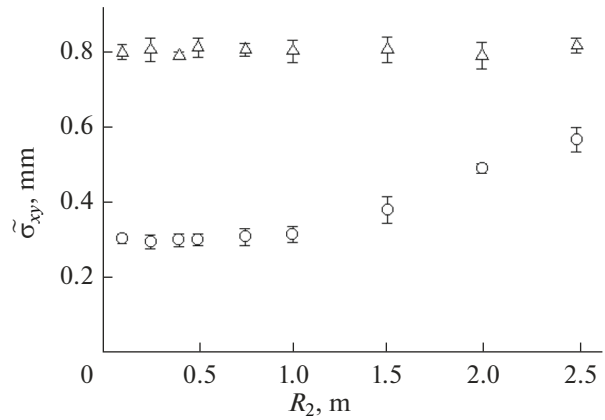

Fig. 2. Dependence of the obtained estimates of the electron-beam dimensions on the crystal—detector distances. Points correspond to the size in the horizontal plane. Triangles correspond to the dimensions in the vertical plane.

more smaller than Θ_{ph}, providing approximately the same decrease in the transverse size of the electron beam, which can be measured using the proposed procedure.

To confirm the foregoing, the results of simulating the determination of the size of the 10-GeV electron beam are given in Fig. 3. Simulation was performed under the following conditions including Si crystal (022) reflection and an observation angle of 32.2°. The detector-element dimensions were 10×10 μm for the smaller distance and 20×20 μm for the larger one. The electron-beam dimensions at the crystal were $\sigma_x = 15$ μm and $\sigma_y = 20$ μm. The electron-beam divergence was $\theta_e = 15$ μrad. It is known, for example, [19, 20] that the angular DTR distribution can be represented in the form:

$$Y_{DTR}(\theta_x, \theta_y) = N_{DTR}(\omega)\frac{\theta_x^2 \cos^2 2\Theta_B + \theta_y^2}{((\theta^2 + \Theta_{ph}^2)(\theta^2 + \gamma^{-2}))^2}, \quad (7)$$

where $\theta^2 = \theta_x^2 + \theta_y^2$, and $N_{DTR}(\omega)$ is the factor characterizing the DTR yield, which depends on the observation angle and the photon energy. The contribution of this mechanism was not taken into account because of the small DTR intensity. To obtain the angular radiation distribution from the point electron beam (dependence *2*), distribution *1* was convolved with two-dimensional Gaussian distribution with a divergence angle of $\theta_e = 15$ μrad. Two remaining dependences correspond to the angular distribution for crystal—detector distances of 2 and 1 m (curves (*3*) and (*4*)). To take into account the possible influence of the statistical straggling of the measured data, the dependences for the finite-dimensional beam were made "noisy", as in the calculation of the angular PXR distribution in Fig. 1.

(a)

(b)
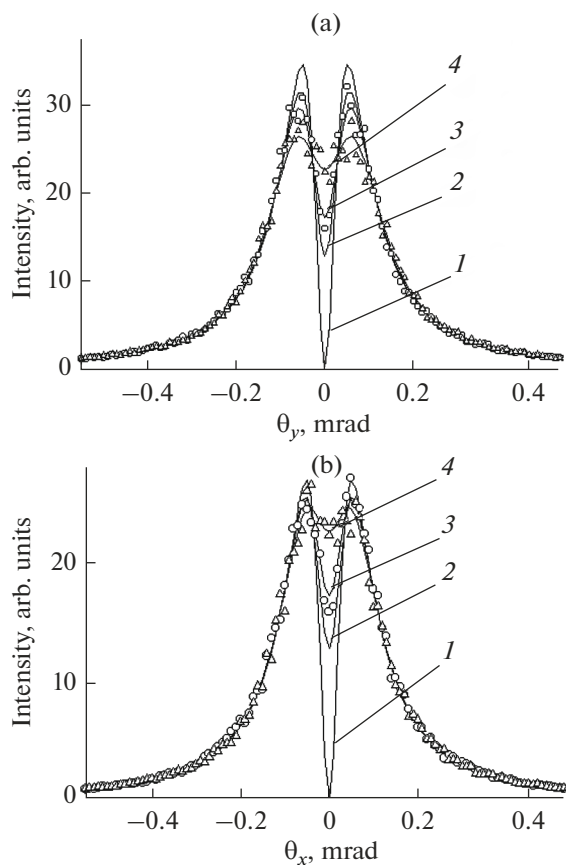
Fig. 3. (a) Vertical and (b) horizontal angular DTR distributions. The curves correspond to (*1*) the calculation using formula (7), (*2*) the distribution for the point electron beam, (*3*) the distribution for the extended beam and a distance of 1 m, and (*4*) the distribution for the extended beam and a distance of 0.5 m. The points correspond to a distance of 2 m; and triangles, to a distance of 1 m.

As in the case of PXR, the error in determining the fitting parameters did not exceed 5−7%, and the "fitted" dependence almost coincided with dependence (*4*) and, therefore, is not given.

To determine the method sensitivity for this radiation mechanism and the electron energy range, we performed a cycle of estimations of the beam dimensions obtained using the proposed given procedure and of "noisy" angular distributions as functions of the crystal—detector distances. Simulation was performed for beam dimensions of $\sigma_x = 20$ μm and $\sigma_y = 30$ μm. The other parameters coincided with those given above. The dependence of the estimates of the beam size $\tilde{\sigma}_{x,y}$ on the distance obtained as a result of fitting is given in Fig. 4. As in the case of PXR, the condition $R_1 = 2R_2$ is satisfied, and the standard deviations of the values obtained as a result of fitting from the average one were used as errors.

It is seen from Fig. 4 that, for crystal—detector distances that were smaller than 2 m, the error in estimat-
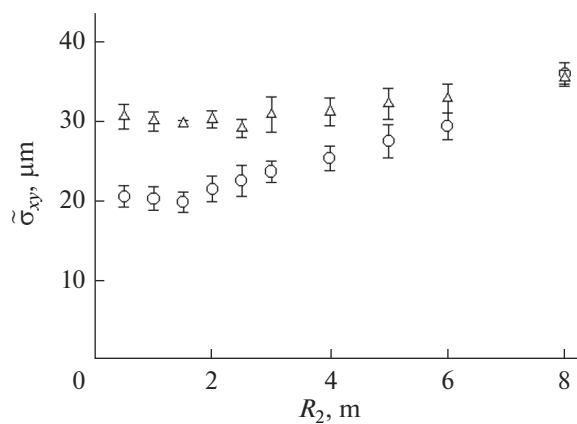

Fig. 4. Dependence of the obtained estimates of the electron-beam dimensions on the crystal—detector distances. Points correspond to the dimensions in the horizontal plane. Triangles correspond to the dimensions in the vertical plane.

ing the beam size did not exceed 5−7%, and the estimates coincide with the values used in the simulation. For larger distances, the difference between the estimate and the beam size increases with increasing distance, as in the PXR case. The difference begins to exceed the standard deviation for R_2 on the order of 2.5 and 5 m for the horizontal and vertical beam dimensions, respectively, in the case where the condition $\sigma'_{x,y} = \sigma_{x,y}/R_2 \leq 0.1\Theta_{ch}$, where $\Theta_{ch} = \gamma^{-1}$ begins to be satisfied. As before, for small σ', there is barely a difference between the distributions for different distances, and the method loses its sensitivity as a result. Here it should be mentioned that the difference begins to be manifested for smaller distances with increasing "noise" level.

The requirement $\sigma_{x,y} > \delta_{x,y}$ is a no less important condition, i.e., the detector size $\delta_{x,y}$ must be comparable with the characteristic beam dimensions at the target $\sigma_{x,y}$. If this condition is not satisfied, then there is no difference between the distributions for different distances. A detector with pixel dimensions of 11.2 × 11.6 μm was used in the mentioned experiment [8]; therefore, we can assume that the minimal, reliably determined beam size is ~10 μm.

The main requirement for successful application of the proposed method for measuring the beam size is the equality of solid angles covered by the detector element for both distances. The departure of secondary electrons and quanta from the element, where the photon interacts with the detector material, to neighboring ones distorts the measured distributions, smoothing them. The influence of the effect is stronger for smaller dimensions of the detector elements; therefore, it is equivalent to an additional increase in the particle-beam dimensions at the crystal.
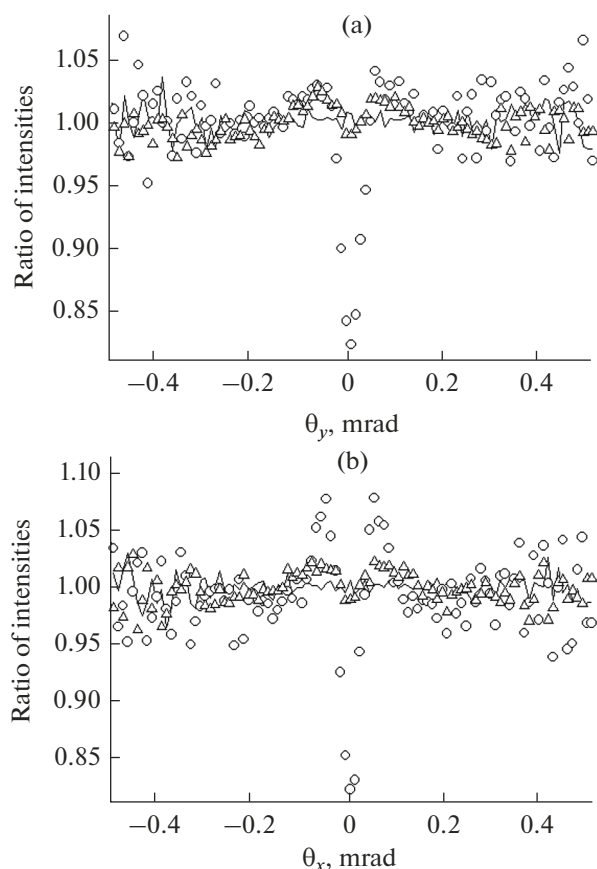
Fig. 5. Ratio of the radiation intensities for the long- and short-range locations of detectors in the (a) vertical and (b) horizontal planes.

To verify the significance of the influence of this effect on the measurement result, we perform simulation of implementation of the procedure with and without inclusion of the influence of the effect of the particle and quantum departure under the following conditions: the electron energy was 10 GeV, the Si crystal orientation was (011), the photon energy was $\omega = 11.65$ keV, and the detector-element dimensions were 10×10 μm and 20×20 μm for the crystal—detector distances of 1 and 2 m. The electron-beam dimensions at the target were 10 μm in the vertical plane and 20 μm in the horizontal one. The electron-beam divergence was 10 μrad. To simplify the simulation process, instead of dependence (7), we used the azimuthally symmetric spectral—angular distribution of the transition radiation, which is often called the Garibian formula [21].

Simulation was performed by means of the Monte Carlo method for the parameters of an HR25 detector [22] used in the experiment [8], where a P43 scintillator with the chemical composition Gd_2SO_2 and a thickness of 30 μm was used. The procedure for simulating the detector parameters was given in [23].

Figure 5 shows the ratio of the radiation intensities recorded by the detector for two distances in the vertical (Fig. 5a) and horizontal (Fig. 5b) planes. Simulation was performed for a point electron beam without considering the detector influence (curve), for a point electron beam with inclusion of the influence of the detector (triangles), and for an extended electron beam without considering the influence of the detector (points).

It follows from Fig. 5 that the angular distributions measured for two distances coincide if the electron-beam dimensions at the target and the influence of the departure of secondary particles and quanta are not considered. For large observation angles, the spread of the values is due to low statistics because of a sharp decrease in the transition-radiation intensity with increasing photon departure angle (Fig. 3). The inclusion of the departure of secondary particles and quanta (triangles) leads to a certain difference between the angular distributions at different distances; but this difference is rather small and does not exceed several percent, which is close to the statistical straggling.

The influence of the beam size at the crystal (points) is considerably more significant. The deviation of the ratio of the radiation intensities from unity reaches 15% or more. The electron-beam dimensions in the vertical and horizontal planes are different; therefore, the ratio of intensities recorded by the detector for two different distances are also different in the vertical and horizontal planes; our proposed method for determining the electron-beam dimensions in both planes is based precisely on this fact. Simultaneous inclusion of the beam dimensions at the target and the influence of the departure of secondary electrons and quanta barely changed the ratio of the radiation intensities as compared with the results of the simulation, where the secondary radiation departure was not taken into account. Therefore, this dependence is not given here.

Consequently, for photon energies of about 10 keV and detector pixel dimensions on the order of 10 μm, the influence of the departure of secondary particles and quanta during the process of X-ray radiation recording comparatively weakly affects the results of measuring the beam dimensions by means of the proposed procedure and (in the first approximation) can be not considered.

In the X-ray frequency range, free-electron lasers [15] operate up to wavelengths of ~0.1 nm, which corresponds to a photon energy of ~15 keV. Thus, the wavelength chosen to verify the method applicability is comparable with the longitudinal bunch dimensions, which is insufficient for the exclusion of coherent effects in the radiation. In the case of implementation of the free-electron laser, the transverse electron-beam dimensions are on the order of 100 μm or higher,

which makes it possible to increase the photon energy by decreasing the observation angle and preserving a rather large distance between the electron beam and the detector axis, which is required to protect the detector from the background, by increasing the distance between the crystal and the coordinate detector.

It is possible to decrease the radiation wavelength tenfold or more, because the PXR and the DTR of photons with an energy of $\omega \sim 145$ keV was reliably recorded for an observation angle of $4°$ in the experiment [20]. An increase in the recorded photon energy can lead to an increase in the influence of the departure of secondary particles and quanta and requires in-depth analysis, which takes into account the energy of recorded photons, the characteristics of the chosen detector, and other experimental factors.

CONCLUSIONS

The transverse dimensions of the particle beam $\sigma_{x,y}$ can be determined using the results of measuring the angular (spatial) radiation distributions for fast electrons in thin crystals for two different distances between the source and the coordinate detector. The sought beam dimensions were determined by the fitting of the distribution for a smaller distance using the convolution of the distribution for a larger distance and the two-dimensional Gaussian one, whose parameters are unambiguously related to the beam dimensions and the crystal—detector distances. The method applicability limit is the condition $\sigma_{x,y}/R > 0.1\Theta_{ch}$. For the PXR mechanism, the characteristic angle Θ_{ch} coincided with Θ_{ph}, and was close to γ^{-1} for thin crystals and electron energies that are higher than several gigaelectronvolts. For photon energies on the order of 10 keV and a coordinate detector element size of 10×10 μm, the influence of the effect of departure of secondary electrons and photons from the pixel, where X-ray photons interact with the detector, to the neighboring ones was small and can be not considered in the first approximation.

An additional requirement is the validity of the condition for the relation between the characteristic beam size to the detector size $\sigma \sim \delta$. The simultaneous validity of both requirements restricts the measured beam size to a value of $60-100$ μm for the PXR mechanism and an electron energy of at most 1 GeV and to a value of $10-15$ μm for the DTR mechanism and an electron energy of several gigaelectronvolts or more. The method can also be used for intermediate electron energies in the cases where there is no dominant type of radiation. For this reason, it is difficult to determine its sensitivity range. Calculations taking into account the contributions of all mechanisms, the crystal thickness, and other experimental conditions are required.

If it is necessary to measure the parameters of beams with bunch lengths on the order of 0.1 nm or less, it is possible to use smaller observation angles and larger photon energies, which leads to an increase in the effect of the influence of the departure of secondary particles and quanta from the point where photons interact with the detector material to neighboring pixels. This problem requires more profound analysis, results of which will be given in the following papers.

The proposed procedure for estimating electron beam dimensions is model-independent and does not require exact knowledge of the beam divergence and the degree of crystal-structure perfection. The main requirement is the identity of the angular radiation distributions in measurements for different crystal—detector distances. The procedure is slightly sensitive to pulsed heating of the target if it does not lead to crystal destruction [24] and can be used in the case of intense beams of linear accelerators for free-electron X-ray lasers.

REFERENCES

1. R. Fulton, J. Haggerty, R. Jared, R. Jones, P. Kadyk, C. Field, W. Kozanecki, and W. Koska, Nucl. Instrum. Methods Phys. Res., Sect. A **274,** 37 (1989).

2. M. Harrison et al., in *FEL2013: Proceedings of the 35th Free-Electron Laser Conference (New York, August 26–30, 2013)* (JACoW, Manhattan, NY, USA, 2013), p. 276.

3. R. B. Fiorito, in *Proceed. Particle Accelerator Conf. Vancouver* (2009), p. 741.

4. J. Urakawa, H. Hayano, K. Kubo, et al., Nucl. Instrum. Methods Phys. Res., Sect. A **472,** 309 (2001).

5. H. Loos, R. Akre, F. -J. Decker, et al., in *Proceed. 30th Int. Free Electron Laser Conf.* (Gyeongju, 2008), p. 485.

6. A. Gogolev, A. Potylitsyn, and G. Kube, J. Phys.: Conf. Ser. **357,** 012018 (2012).

7. Y. Takabayashi, Phys. Lett. A **376,** 2408 (2012).

8. G. Kube, C. Behrens, A. S. Gogolev, et al., in *Proceed. Int. Particle Accelerator Conf.* (Pasadena, 2013), p. 491.

9. Y. Takabayashi and K. Sumitani, Phys. Lett. A **377,** 2577 (2013).

10. I. E. Vnukov, Yu. A. Goponov, M. A. Sidnin, R. A. Shatokhin, K. Sumitani, and Y. Takabayashi, J. Surf. Invest.: X-ray, Synchrotron Neutron Tech. **13** (3), 515 (2019).

11. S. A. Laktionova, O. O. Pligina, M. A. Sidnin, et al., J. Phys.: Conf. Ser. **517,** 012020 (2014).

12. Y. Takabayashi and A. V. Shchagin, Nucl. Instrum. Methods Phys. Res., Sect. B **272,** 78 (2012).

13. Y. Takabayashi, K. B. Korotchenko, Yu. V. Pivovarov, et al., Nucl. Instrum. Methods Phys. Res., Sect. B **202,** 79 (2017).

14. I. D. Feranchuk and A. V. Ivashin, J. Phys. (Paris), **46**, 1981 (1985).

15. *The European X-Ray Free-Electron Laser. Technical Design Report,* Ed. by M. Altarelli, R. Brinkmann, M. Chergui, (DESY, Hamburg, 2006).

16. Yu. A. Goponov, S. A. Laktionova, O. O. Pligina, et al., Nucl. Instrum. Methods Phys. Res., Sect. B **355,** 150 (2015).

17. Yu. A. Goponov, M. A. Sidnin, K. Sumitani, Y. Takabayashi, and I. E. Vnukov, Nucl. Instrum. Methods Phys. Res., Sect. A **808,** 71 (2016).

18. I. Chaikovska, R. Chehab, X. Artru, and A. V. Shchagin, Nucl. Instrum. Methods Phys. Res., Sect. B **402,** 75 (2017).

19. A. P. Potylitsin and V. A. Verzilov, Phys. Lett. A **209,** 380 (1995).

20. A. N. Baldin, I. E. Vnukov, B. N. Kalinin, et al. J. Surf. Invest.: X-Ray Synchrotron Neutron Tech., No. 4, 72 (2006).

21. G. M. Garibyan and Y. Shi, *X-Ray Transition Radiation* (Izd. Akad. Nauk Arm. SSR, Erevan, 1983) [in Russian].

22. X-Ray camera. http://www.proxivision.de/datasheets/X-Ray-Camera-HR25-x-ray-PR-0055E-03.pdf

23. Yu. A. Goponov, S. A. Laktionova, M. A. Sidnin, et al., Nucl. Instrum. Methods Phys. Res., Sect. B **402,** 92 (2017).

24. A. A. Babaev and A. S. Gogolev, J. Phys.: Conf. Ser. **732,** 012030 (2016).

Translated by L. Kulman